

Figure 7. Luminescence spectra for selective excitation ( $14862\text{ cm}^{-1}$ ) of site A at two temperatures. The lines are denoted as in Figure 6.

in the wings of the main lines A and B, or even sites that are not detectable in the absorption spectrum, contributing less than 1% to the total intensity. Table III contains the results of a few selected majority and minority sites. The observed inhomogeneous broadening and the presence of minority sites demonstrate that the crystal is by no means perfect. The broadening is similar for sites A and B at 1.5 K. However, as shown in Figure 3, the widths of the site B bands increase much more strongly than those of site A.

The ground-state exchange splittings for all the sites resemble the Landé pattern expected for a Heisenberg Hamiltonian rather closely. Accordingly, the biquadratic exchange parameters are small, approximately 1% of  $2J$ . Exchange parameter values for the various sites are collected in Table III. These values are very accurate, and they show little variation. In particular, the parameters are the same for the majority sites A and B. This is interesting, because there is a significant difference in the anisotropy parameters  $D$  and  $E$  between the two sites. We have attributed this difference to a geometrical distortion or a different crystal environment of site A. The exchange parameters are obviously not affected by this. Exchange parameters of minority sites outside the main absorption band profile show deviations of up to  $\pm 5\%$  from those of the majority sites. An extreme outsider is the site with a  ${}^5B_1 \rightarrow {}^5A_1$  luminescence energy  $34\text{ cm}^{-1}$  above the majority sites A. It has a  $J$  value of  $16.1\text{ cm}^{-1}$  compared to  $15.3\text{ cm}^{-1}$  for the majority sites.

The spectra in Figure 6 clearly show that there is no transfer of excitation energy between the sites at 1.5 K. This is no longer

true at higher temperatures, as illustrated in Figure 7. At 34 K selective excitation of site A results in a superposition of luminescence from both sites. Excitation energy is nonradiatively transferred from site A to site B. The process is thermally activated. We have investigated this phenomenon and the possible underlying mechanisms in detail, and a full account of this work is published elsewhere.<sup>12</sup>

### Conclusions

We have shown by single-crystal absorption and Zeeman spectroscopy that the published crystal structure of  $[(\text{NH}_3)_5\text{CrOHCr}(\text{NH}_3)_5]\text{Cl}_5 \cdot \text{H}_2\text{O}$  can only be an approximation. It was determined on the basis of single-crystal X-ray diffraction data and refined to a  $R$  value of 0.077. A structural phase transition between room temperature and 1.5 K can be ruled out as a reason for the discrepancy between the spectroscopic and X-ray results on the basis of the room-temperature absorption spectrum. The existence of two crystallographically nonequivalent sites is clearly established by the spectroscopy, and the orientation of both sites in the crystal determined. Site B corresponds to the X-ray position, whereas site A is tilted by  $90 \pm 10^\circ$  around the molecular  $y$  axis from that orientation. High-resolution optical spectroscopy proves to be a very sensitive structural probe in this situation. In addition, it allows the determination of molecular parameters for each individual site in the crystal. The main focus in this study was on the ground-state exchange splitting of the  $[(\text{NH}_3)_5\text{CrOHCr}(\text{NH}_3)_5]^{5+}$  units. The exchange parameters of the majority sites are in exact agreement with those determined on the deuterated compound at 30 K by another spectroscopic technique, inelastic neutron scattering (INS).<sup>15</sup> The spectral resolution of the optical spectroscopic results at 1.5 K presented here is approximately 1 order of magnitude better than the INS resolution in ref 15. In contrast to INS, optical spectroscopy provides selectivity. It has the additional advantage that the transfer of excitation energy can be investigated, thus providing information about intermolecular interactions. It turns out to be a highly sensitive and selective technique for probing both electronic excitations and structural properties.

**Acknowledgment.** We thank N. Furrer and P. Küng for their assistance with the synthesis and crystal growth. Financial support by the Swiss National Science Foundation is gratefully acknowledged.

**Registry No.**  $[(\text{NH}_3)_5\text{CrOHCr}(\text{NH}_3)_5]\text{Cl}_2 \cdot \text{H}_2\text{O}$ , 15629-41-1.

(15) Güdel, H. U.; Furrer, A. *Mol. Phys.* 1977, 33, 1335.

Contribution from the Service d'Etudes Analytiques and the Département de Recherche Fondamentale, Centre d'Etudes Nucléaires de Grenoble, 85 X, 38041 Grenoble Cedex, France

## Desorption Chemical Ionization Mass Spectrometry via Electron Capture of Hydrolytically Labile Titanium Porphyrins

E. Forest,<sup>†</sup> J. C. Marchon,<sup>\*†</sup> J. Ulrich,<sup>†</sup> and H. Virelizier<sup>§</sup>

Received February 12, 1986

A comparison of electron impact ionization (EI), fast atom bombardment (FAB), and desorption chemical ionization (DCI) mass spectrometry of dihalogenotitanium(IV) porphyrins shows that DCI in the electron capture mode is uniquely suited to the production of abundant molecular ions for this class of hydrolytically labile coordination complexes.

The mass spectrometric characterization of metalloporphyrin complexes<sup>1</sup> is often plagued by the cleavage of their axial metal-ligand bonds. Thus, the highest peaks in the mass spectra of five- and six-coordinate porphyrin complexes usually correspond to the molecular ion of the four-coordinate metalloporphyrin or

to that of a hydrolytically produced oxo complex. The difficulties in obtaining accurate structural and molecular weight information

- (1) For recent advances in this field, see: (a) Kurlansik, L.; Williams, T. J.; Strong, J. M.; Anderson, L. W.; Campana, J. E. *Biomed. Mass Spectrom.* 1984, 11, 475-481. (b) Sundararaman, P.; Gallegos, E. J.; Baker, E. W.; Slayback, J. R. B.; Johnston, M. R. *Anal. Chem.* 1984, 56, 2552-2556. (c) Fukuda, E. K.; Campana, J. E. *Anal. Chem.* 1985, 57, 949-952. (d) Chait, B. T.; Field, F. H. *J. Am. Chem. Soc.* 1984, 106, 1931-1938. (e) Freas, R. B.; Campana, J. E. *Inorg. Chem.* 1984, 23, 4654-4658.

<sup>†</sup>Service d'Etudes Analytiques (CEA/IRDI), CEN de Grenoble.

<sup>†</sup>Département de Recherche Fondamentale (DRF/LCH), CEN de Grenoble.

<sup>§</sup>Service d'Etudes Analytiques (CEA/IRDI), CEN de Saclay.

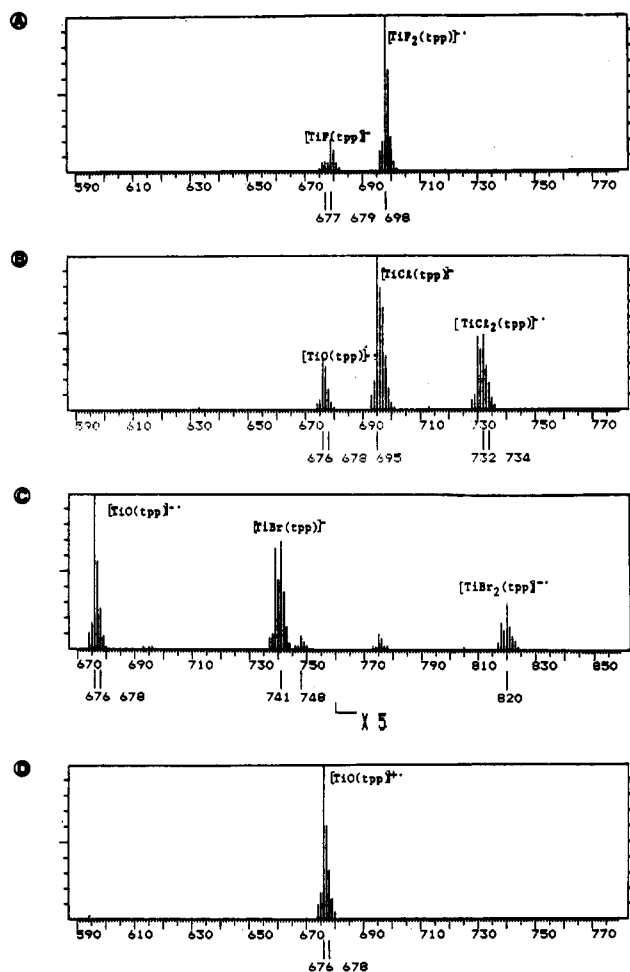


**Figure 1.** DCI mass spectra of titanium(IV) tetraphenylporphyrin complexes: (A) negative-ion spectrum of  $\text{TiF}_2(\text{tpp})$  (molecular ion observed at  $m/z$  698, with smaller peaks at  $m/z$  679 ( $[\text{TiF}(\text{tpp})]^-$ ) and  $m/z$  676 ( $[\text{TiO}(\text{tpp})]^-$ ); (B) negative-ion spectrum of  $\text{TiCl}_2(\text{tpp})$  (significant loss of a chlorine atom ( $[\text{TiCl}(\text{tpp})]^-$ ,  $m/z$  695), and hydrolysis ( $[\text{TiO}(\text{tpp})]^-$ ,  $m/z$  676) observed); (C) negative-ion spectrum of  $\text{TiBr}_2(\text{tpp})$  (note the extensive loss of bromine atom and hydrolysis); (D) positive-ion spectrum of  $\text{TiO}(\text{tpp})$ .

on this class of complexes are exemplified by the behavior of tetraphenylporphyrin (tpp) complexes of iron(III) and titanium(IV): electron impact ionization (EI) spectra of  $\text{FeCl}(\text{tpp})$  and  $\text{FeBr}(\text{tpp})$  exhibit peaks of  $[\text{Fe}(\text{tpp})]^+$  as the most abundant ion (following loss of the halogen atom), while those of  $\text{TiX}_2(\text{tpp})$  (where  $X = \text{F}, \text{Cl}, \text{or Br}$ ) all yield  $[\text{TiX}(\text{tpp})]^+$  and  $[\text{TiO}(\text{tpp})]^+$  (following hydrolysis of the metal-halogen bonds<sup>2,3</sup>). We have investigated soft ionization techniques (DCI, desorption chemical ionization,<sup>4</sup> and FAB, fast atom bombardment<sup>5</sup>) to circumvent these problems, and we report herein that DCI in the electron

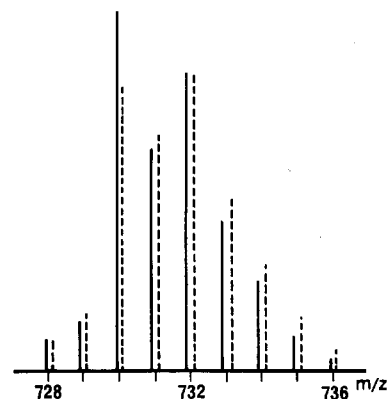


**Figure 2.** Calculated (solid line) vs. observed (dotted line) isotopic distribution patterns for the  $[\text{TiCl}_2(\text{tpp})]^-$  molecular ion.

capture mode gives accurate molecular weight results for the series of dihalogenotitanium(IV) complexes.

DCI mass spectra<sup>6</sup> in the electron capture mode for  $\text{TiX}_2(\text{tpp})$  ( $X = \text{F}, \text{Cl}, \text{Br}$ ) are shown in Figure 1; the positive-ion spectrum of  $\text{TiO}(\text{tpp})$  is also shown for comparison. The most abundant peaks in the spectrum of  $\text{TiF}_2(\text{tpp})$  are those of the molecular ion ( $m/z$  698). Smaller peaks at  $m/z$  679 and 676 reveal the formation of  $[\text{TiF}(\text{tpp})]^-$  and  $[\text{TiO}(\text{tpp})]^-$  in small amounts. By contrast, the positive-ion DCI, EI, and FAB (*p*-nitrobenzyl alcohol matrix) spectra of this complex exhibit predominant  $[\text{TiO}(\text{tpp})]^+$  peaks and very weak peaks for  $[\text{TiF}_2(\text{tpp})]^+$ . The DCI mass spectrum (electron capture mode) of  $\text{TiCl}_2(\text{tpp})$  shows predominant peaks for  $[\text{TiCl}(\text{tpp})]^-$ , with molecular ion peaks for  $[\text{TiCl}_2(\text{tpp})]^-$  more abundant than those of the hydrolytic product  $[\text{TiO}(\text{tpp})]^-$ . The spectrum of  $\text{TiBr}_2(\text{tpp})$  is consistent with the trend ( $\text{F} > \text{Cl} > \text{Br}$ ) observed in the solution hydrolytic stability of this series of complexes,<sup>2</sup> but the molecular ion peaks are still easily observed (Figure 1).

A comparison of the experimental and calculated isotopic distribution patterns for the molecular ion of  $\text{TiCl}_2(\text{tpp})$  is shown in Figure 2. The fair agreement that is obtained confirms the assignment of the peaks as those of the molecular ion. It also confirms the soft character of the DCI technique, which, in the electron capture mode, is uniquely suited to the production of abundant molecular ions and avoids extensive fragmentation and hydrolysis for this class of complexes.<sup>7</sup> By comparison, molecular ion peaks are not observed in EI and FAB mass spectra of  $\text{TiCl}_2(\text{tpp})$  and  $\text{TiBr}_2(\text{tpp})$ ; the soft character of the FAB ionization technique is probably offset by preliminary reactions with the liquid matrix (hydrolysis, axial ligand substitution by *p*-nitrobenzyl alcohol) in these instances.

In summary, desorption chemical ionization mass spectrometry has readily provided the molecular ions of easily hydrolyzed dihalogenotitanium(IV) porphyrin complexes, which are difficult to obtain by other ionization techniques. This result suggests that DCI might constitute a significant development in the ability to characterize thermally and/or hydrolytically labile metal complexes and organometallic compounds. In the present study, the chemical stability of the one-electron-reduced complex<sup>9</sup> is probably

(2) Nakajima, M.; Latour, J. M.; Marchon, J. C. *J. Chem. Soc., Chem. Commun.* **1977**, 763-764.

(3) Lecomte, C.; Protas, J.; Marchon, J. C.; Nakajima, M. *Acta Crystallogr., Sect. B: Struct. Crystallogr. Cryst. Chem.* **1978**, *B34*, 2856-2858.

(4) Cotter, R. J. *Anal. Chem.* **1980**, *52*, 1589A-1606A.

(5) For recent advances in FAB mass spectrometry of metal complexes, see: (a) Finke, R. G.; Droegge, M. W.; Cook, J. C.; Suslick, K. S. *J. Am. Chem. Soc.* **1984**, *106*, 5750-5751. (b) Tkatchenko, I.; Niebecker, D.; Fraisse, D.; Gomez, F.; Barofsky, D. F. *Int. J. Mass Spectrom. Ion Phys.* **1983**, *46*, 499-502. (c) Johnstone, R. A. W.; Lewis, I. A. S. *Int. J. Mass Spectrom. Ion Phys.* **1983**, *46*, 451-454. (d) Barber, M.; Bordoli, R. S.; Sedgwick, R. D.; Tyler, A. N. *Biomed. Mass Spectrom.* **1981**, *8*, 492-495. (e) Cerny, R. L.; Sullivan, B. P.; Bursey, M. M.; Meyer, T. J. *Anal. Chem.* **1983**, *55*, 1954-1958. (f) Davis, R.; Groves, I. F.; Durrant, J. L. A.; Brooks, P.; Lewis, I. *J. Organomet. Chem.* **1983**, *241*, C27-C30. (g) Miller, J. M. *J. Organomet. Chem.* **1983**, *249*, 299-302. (h) Cerny, R. L.; Bursey, M. M.; Jameson, D. L.; Malachowski, M. R.; Sorrell, T. N. *Inorg. Chim. Acta* **1984**, *89*, 89-93. (i) Miller, J. M.; Fulcher, A. *Can. J. Chem.* **1985**, *63*, 2308-2312.

(6) All DCI mass spectra (positive-ion or electron capture modes), were obtained on a NERMAG R-1010 quadrupole mass spectrometer controlled by a PDP 8M computer. Microgram samples were dissolved in a few microliters of  $\text{CHCl}_3$ , and this solution was deposited on the filament. The current was varied from 100 to 700 mA at a rate of 10 mA/s. The peak at  $m/z$  633 of perfluorotributylamine was used for adjustment of the source and for calibration. Reactant gases were ammonia or methane.

(7) There are very few reported examples where negative ionization gives better results than positive ionization in DCI mass spectrometry.<sup>8</sup> In the present study, the success of electron capture DCI probably derives from the chemical stability of the dihalogenotitanium(III) complexes  $[\text{TiX}_2(\text{tpp})]^{2-}$ .

(8) Virelizier, H.; Hagemann, R.; Jankowski, K. *Biomed. Mass Spectrom.* **1983**, *10*, 559-566.

(9) Latour, J. M.; Marchon, J. C.; Nakajima, M. *J. Am. Chem. Soc.* **1979**, *101*, 3974-3976.

crucial for the success of the electron capture mode. Investigation of other classes of complexes that exhibit a stable lower oxidation state will be necessary, however, before the generality of this observation can be established.

**Acknowledgment.** We thank the CNRS (Unité Associée No.

1194: Laboratoire de Chimie de Coordination) for partial support of this research and Dr. Jean-Marc Latour for several interesting discussions.

**Registry No.**  $\text{TiF}_2(\text{tpp})$ , 66350-84-3;  $\text{TiCl}_2(\text{tpp})$ , 66350-83-2;  $\text{TiBr}_2(\text{tpp})$ , 66350-82-1;  $\text{TiO}(\text{tpp})$ , 58384-89-7.

Contribution from the Departments of Chemistry, University of Notre Dame, Notre Dame, Indiana 46556, and The Ohio State University, Columbus, Ohio 43210

## Substituent Effects in Clusters. 5. UV-Photoelectron Spectroscopic and Quantum-Chemical Analyses of $\text{H}_3\text{Os}_3(\text{CO})_9\text{BCO}$ , $\text{H}_2\text{Os}_3(\text{CO})_9\text{CCO}$ , and Related Clusters

R. D. Barreto,<sup>†</sup> T. P. Fehlner,<sup>\*†</sup> L.-Y. Hsu,<sup>†</sup> D.-Y. Jan,<sup>†</sup> and S. G. Shore<sup>\*†</sup>

Received January 14, 1986

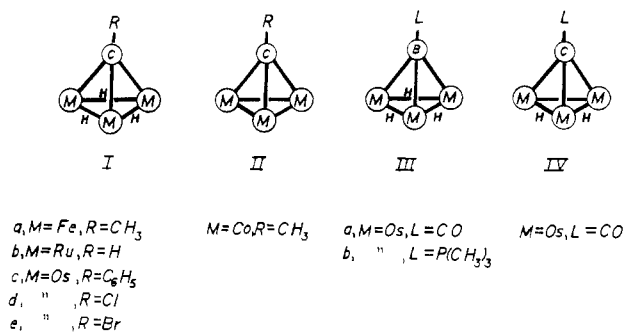
The gas-phase UV-photoelectron spectra of  $(\mu\text{-H})_3\text{Os}_3(\text{CO})_9\text{BL}$  ( $\text{L} = \text{CO}, \text{P}(\text{CH}_3)_3$ ) (IIIa,b),  $(\mu\text{-H})_2\text{Os}_3(\text{CO})_9\text{CCO}$  (IV), and  $(\mu\text{-H})_3\text{Os}_3(\text{CO})_9\text{CX}$  ( $\text{X} = \text{C}_6\text{H}_5, \text{Cl}, \text{Br}$ ) (Ic-e) were measured by using He I radiation with the spectra of Ic and IIIa also being measured with Ne radiation. The observed bands were assigned by comparison to model compounds, intensity changes with photon energy, and exo-cluster substituent effects. The empirical results on IIIa,b and IV are intercompared in order to probe the bonding of the main-group atom to the  $\text{Os}_3$  triangle and the interaction of CO and  $\text{P}(\text{CH}_3)_3$  with a capping boron atom. Molecular orbital calculations of the Fenske-Hall type were carried out for the same molecules. The information gained is consistent with that derived from the spectroscopic work and gives further informative details of the electronic structure. Both the PES results and the MO calculations suggest that boron is acting as a pseudo metal cluster atom relative to the metal centers as well as to attached ligands.

The comparison of spectroscopic properties of isoelectronic molecules is a classical method for obtaining information on the corresponding electronic structures. Indeed such comparisons also constitute a body of data of significant pedagogical value. Although nowadays small molecule problems are effectively treated with modern quantum-chemical techniques, large systems, e.g., transition-metal clusters, are not easily dealt with. In a continuing effort we have pointed out the usefulness of comparing isoelectronic molecules that differ only in the spatial location of a proton.<sup>1</sup> The differences in spectroscopic properties can be related straightforwardly to the perturbation of the electronic structure caused by the proton. For example, the comparison of  $\text{H}_3\text{Fe}_3(\text{CO})_9\text{CCH}_3$  (Ia) with  $\text{Co}_3(\text{CO})_9\text{CCH}_3$  (II) (Chart I) provided a means for probing the metal-metal interactions in the capped trinuclear metal cluster system.<sup>1b,c</sup>

The recent preparation of the first borylydne transition-metal cluster compound,  $\text{H}_3\text{Os}_3(\text{CO})_9\text{BCO}^2$  (IIIa), along with the existing isoelectronic counterpart,  $\text{H}_2\text{Os}_3(\text{CO})_9\text{CCO}^3$  (IV), allows the capped trinuclear metal cluster system to be further investigated. In going from IIIa to IV, a proton is formally moved from a M-M edge to the nucleus of the capping atom. With the understanding gained already from Ia and II, the comparison of IIIa and IV provides a source of information on the capping-atom-metal-triangle interaction. Further, as the CO ligand on the capping boron of IIIa has been replaced by a phosphine,<sup>2</sup> an opportunity is presented for exploring to what extent boron behaves as a pseudometallic cage atom. That is, are the interactions of L with the boron of IIIa,b essentially similar to or different from those of L with an osmium atom?

To explore the electronic structures of IIIa and IV, two techniques are utilized. First, UV-photoelectron (PE) spectroscopy provides an exact, but not detailed, look at some properties of the lowest lying radical-cation states of the molecule. By the use of the spectra of model compounds, spectra at two different photon energies, and exo-cluster substituent effects, the pertinent bands in the spectra are assigned.<sup>4</sup> The results are presented in the language of the LCAO MO model by using Koopmans' theorem<sup>5</sup> but in no way depend on the validity of the model or the theorem.

Chart I



Second, IIIa and IV are also examined by using the Fenske-Hall technique, a nonparametrized, self-consistent-field MO method.<sup>6</sup> This allows a more detailed, but approximate, examination of these molecules. For both approaches the emphasis is on relative comparisons, viz. IIIa and IV, and thus the problems associated with absolute measurements or calculations are largely avoided.

### Photoelectron Spectroscopic Results

**General Band Assignment of IIIa.** The PE spectrum of IIIa is shown in Figure 1A, and the numerical data are summarized

- (1) (a) Wong, K. S.; Dutta, T. K.; Fehlner, T. P. *J. Organomet. Chem.* **1981**, *215*, C48. (b) DeKock, R. L.; Wong, K. S.; Fehlner, T. P. *Inorg. Chem.* **1982**, *21*, 3203. (c) DeKock, R. L.; Deshmukh, P.; Fehlner, T. P.; Housecroft, C. E.; Plotkin, J. S.; Shore, S. G. *J. Am. Chem. Soc.* **1983**, *105*, 815. (d) Vites, J. C.; Housecroft, C. E.; Jacobsen, G. B.; Fehlner, T. P. *Organometallics* **1984**, *3*, 1591.
- (2) Shore, S. G.; Jan, D.-Y.; Hsu, L.-Y.; Hsu, W.-L. *J. Am. Chem. Soc.* **1983**, *105*, 5923.
- (3) Shapley, J. R.; Strickland, D. S.; St. George, G. M.; Churchill, M. R.; Bueno, C. *Organometallics* **1983**, *2*, 185.
- (4) (a) Turner, D. W.; Baker, C.; Baker, A. D.; Brundle, C. R. *Molecular Photoelectron Spectroscopy*; Wiley: New York, 1970. (b) Rabalais, J. W. *Principles of Ultraviolet Photoelectron Spectroscopy*; Wiley-Interscience: New York, 1977.
- (5) Koopman, T. *Physica (Amsterdam)* **1934**, *1*, 104.
- (6) (a) Hall, M. B.; Fenske, R. F. *Inorg. Chem.* **1972**, *11*, 768. (b) Hall, M. B. Ph.D. Thesis, University of Wisconsin, Madison, WI, 1971. (c) Fenske, R. F. *Pure Appl. Chem.* **1971**, *27*, 61.

<sup>†</sup> University of Notre Dame.

<sup>†</sup> The Ohio State University.